Available online at www.sciencedirect.com
ScienceDirect
Trans. Nonferrous Met. Soc. China 20(2010) 1392−1396
Transactions of Nonferrous Metals Society of China
www.tnmsc.cn

Influence of plasma-MIG welding parameters on aluminum weld porosity by orthogonal test

BAI Yan(白 岩)[1], GAO Hong-ming(高洪明)[2], WU Lin(吴 林)[2], MA Zhao-hui(马朝晖)[1], CAO Neng(曹 能)[1]

1. Institute for Welding and Surface Technology of R&D Center, Baoshan Iron & Steel Co. LTD, Shanghai 201900, China;
2. State Key Lab of Advanced Welding Production Technology, Harbin Institute of Technology, Harbin 150001, China

Received 3 August 2009; accepted 28 October 2009

Abstract: The plasma-MIG welding torch was developed. 5A06 aluminum alloys with V-grooves were welded in a single pass in the plasma-MIG welding process and the joints were examined by X-ray diffractometry analysis and mechanical tests. The orthogonal experimental design was used to study the influence of plasma-MIG welding parameters on the aluminum weld porosity. The mixed orthogonal matrix $L_{16}(4^4\times2^3)$ and analysis of variance (ANOVA) technique were employed to optimize the welding parameters. The experimental results indicate that the effect of plasma gas flow rate is dominant, the secondary factors are MIG welding voltage, welding speed, wire feed rate and plasma current in turn. Confirmation experiments were conducted under optimum conditions and there was almost no porosity in the welded joints, thus good mechanical performance joints were obtained.
Key words: plasma-MIG welding; porosity; 5A06 aluminum alloy; orthogonal experimental design

1 Introduction

The plasma-MIG welding process first invented and studied by ESSERS et al[1−2] in Philips Research Laboratories can be regarded as a synthesis of plasma welding and metal inert gas (MIG) welding (Fig.1), which is superior to regular MIG welding process in many aspects such as high welding efficiency, less welding spatter and low porosity sensitivity. The essential feature of the process is that the filler wire and its arc are surrounded by a thermally ionized gas stream, which provides better control of metal and heat transfer to the workpiece[3].

The plasma-MIG welding process covered only experiments with electrodes negative, but it was found that the process is more flexible and stable at positive polarity afterwards. Although the instability at negative polarity could be improved by injecting some oxygen in the argon plasma, the positive mold has been the main subject of further investigations[4−5]. Two types of arcs were observed: a stationary narrow arc with high energy density and a rotating mode with low mean energy density above a critical value of the current through the wire. The narrow arc can be used for deep-penetration welding of thick material or for high-speed welding of thin plate. With the rotating arc, a low-penetration flat weld bead is formed. This could be used for overlying metal substrates with abrasion-resistant or corrosion-resistant coatings[6]. ESSERS et al[7] described the electrical properties of the plasma-MIG system and studied the metal transfer using high-speed photography. Studies by TON[8] indicated that the hybrid arc included an inner jet of argon, metal vapor and an outer stream of argon atoms, ions and electrons. The temperature of the inner arc is about 7 000 K and the outer is about 13 000 K, only a little proportion of the wire current flows through the inner arc.

Plasma-MIG welding process was suitable and successfully applied in welding aluminum such as tank trailers and tubes to flanges[9−11]. However, there is little research on the influence of welding parameters on aluminum weld porosity in plasma-MIG welding process. In this work, the plasma-MIG welding torch is developed independently, 5A06 aluminum alloy is welded and the weld joints are examined by X-ray diffractometry and subjected to mechanical tests. The orthogonal test approach is used to study the influence on the porosity and optimal processing parameters are obtained, which is beneficial to improve mechanical properties.

Corresponding author: BAI Yan; Tel: +86-21-26649552; E-mail: bai_yan@baosteel.com
DOI: 10.1016/S1003-6326(09)60310-1

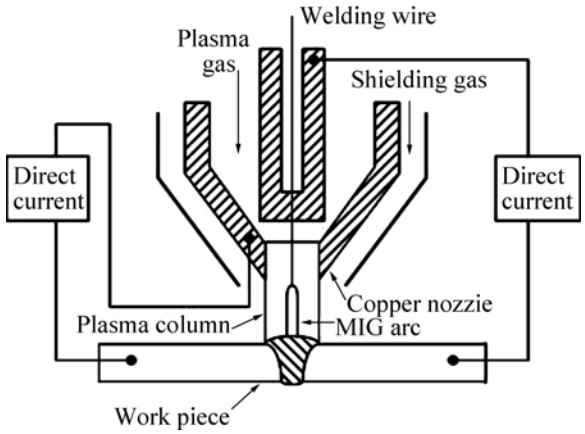

Fig.1 Schematic of plasma-MIG welding process

2 Experimental

The chemical compositions of master alloy and filler wire are listed in Table 1. The size of the specimen is 100 mm×80 mm×10 mm. The 5A06 aluminum alloy with V-groove was welded in a single pass in plasma-MIG welding process. The height of the shoulder was 3 mm. The test pieces were firstly ground using steel brush and sandpaper to remove the oxide film, and then cleaned with acetone to remove the organism such as oily soil.

Table 1 Chemical compositions of 5A06 Al alloy and filler wire (mass fraction, %)

Material	Si	Fe	Cu	Mn	Mg	Ni	Zn	Ti	Al
Master alloy	0.40	0.17	0.07	0.71	5.96	0.01	0.11	0.056	Bal.
Filler wire	<0.40	<0.40	<0.10	0.63	6.20	−	<0.20	0.05	Bal.

After welding, the welded joints were examined by an X-ray diffractometer to quantify the porosity. Some welds were machined to standard test pieces. Tensile tests were carried out at room temperature at a speed of 1 mm/min. The average value of each joint was taken from three tensile specimens cut from the same joint.

3 Experimental

3.1 Index of orthogonal experiment

The weld porosity, which decreases the mechanical properties of welded joints, is one of the main defects in welding aluminum alloys. During the XRD examination, a fixed-length-position weld bead was selected first (Fig.2(a)), then the outlines of the weld beam and the porosities (Fig.2(b)) were obtained through the image processing, at last in the average weld width of upper side and lower side were achieved by calculation to simplify the computation of weld seam area as shown in Fig.2(c). The index of the orthogonal experiment, porosity ratio X_k, can be defined as

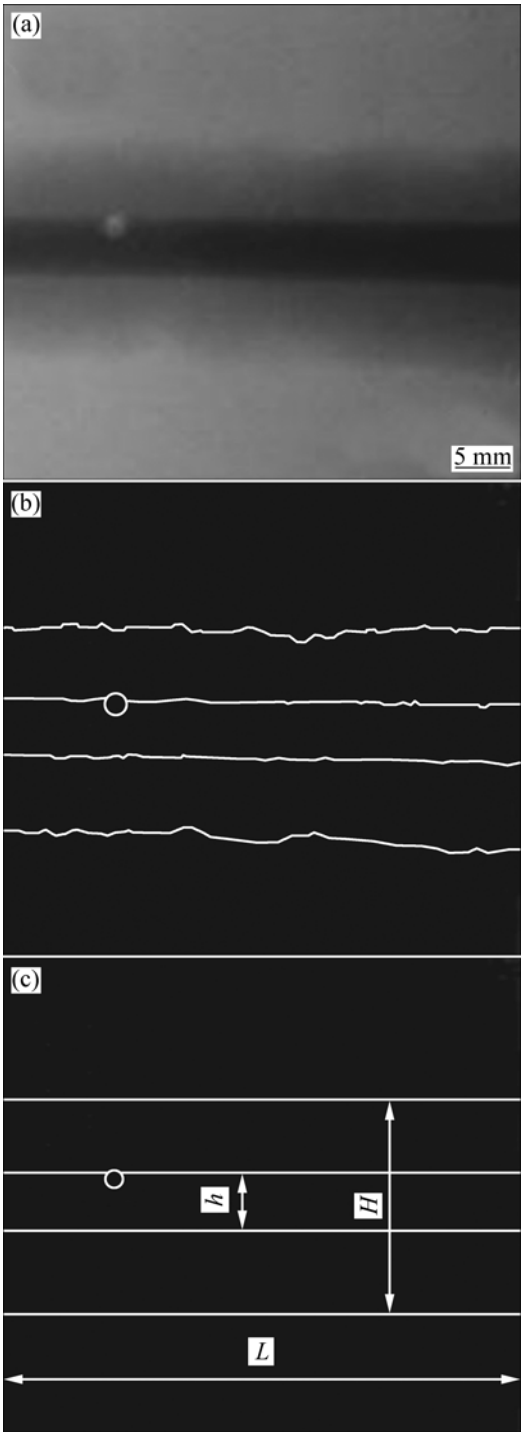

Fig.2 Computation of weld porosity rate: (a) X-ray inspection image; (b) Boundary extraction; (c) Computation of average weld width

$$X_k = \frac{S_p}{S_w} = \frac{\sum S_{pi}}{\frac{(H+h)}{2} \cdot L} \quad (1)$$

where S_p is the sum of porosity in the welded joint, S_w is the area of weld beam, S_{pi} is the area per porosity, H is the average weld width of the upper side, h is the average weld width of the lower side, L is the selected weld length.

3.2 Factors and levels of orthogonal experiment

During the plasma-MIG welding process, some primary welding parameters were taken as the factors of orthogonal experiment, i.e. wire feed rate, MIG welding voltage, plasma welding current, shielding gas (argon) flow rate, plasma gas (argon) flow rate and welding speed. In the present investigation, the levels of factors were restricted in order to obtain full penetrated weld joints. Selected process parameters and their levels in the experiment are shown in Table 2. Other technical parameters used in the study are constant, for example, the distance between the welding torch and test piece B is 10 mm, the inner diameter of water-cooled nozzle R is 10 mm. The mixed-level $L_{16}(4^4\times2^3)$ matrix (Table 3) was employed to examine and optimize the welding parameters in view of the influence of experimental error on the results[12]. In order to estimate the effects of factors after implementing the mixed-level matrix, the analysis of variance (ANOVA) technique was employed, thus, S and F values can be computed. S is defined as the sum of deviation squares, while F shows the significance of factors' influence on the results.

Table 2 Factors and levels of orthogonal experiment

No.	Factor	Level 1	Level 2	Level 3	Level 4
A	Wire feed rate/(m·min^{-1})	9.0	10.1	11.2	12.3
B	MIG welding voltage/V	26.4	28.5	30.2	32.0
C	Plasma current/A	95.0	110.0	125.0	140.0
D	Plasma gas flow rate/(L·min^{-1})	8.0	10.0	−	−
E	Shielding gas flow rate/(L·min^{-1})	20.0	25.0	−	−
F	Welding speed/(mm·min^{-1})	400.0	600.0	−	−

4 Results and discussion

4.1 ANOVA results in orthogonal experiment

16 experimental trials were pre-designed according to the mixed-level $L_{16}(4^4\times2^3)$ array and the corresponding porosity ratio X_k were obtained and listed in Table 3, where K_i are the sum of output response X_k for certain factor at level i, T is the sum of X_k. Because $S_e>>S_E$, S_E can be neglected and the new sum of deviation squares for error $S_{e'}=S_e+S_E$. The results of

Table 3 $L_{16}(4^4\times2^3)$ matrix and experimental results

Experiment No.	A	B	C	D	E	F	Index X_k/%
1	1	1	1	1	1	1	0.823
2	1	2	2	1	2	2	0.617
3	1	3	3	2	1	2	0.217
4	1	4	4	2	2	1	0.373
5	2	1	3	2	2	1	0.083
6	2	2	4	2	1	2	0
7	2	3	1	1	2	2	0.553
8	2	4	2	1	1	1	0.387
9	3	1	3	1	2	2	0.543
10	3	2	4	1	1	1	0.313
11	3	3	2	2	2	1	0.100
12	3	4	1	2	1	2	0.667
13	4	1	2	2	1	2	0.637
14	4	2	1	2	2	1	0.113
15	4	3	4	1	1	1	0.617
16	4	4	3	1	2	2	1.047
K_1	2.030	2.086	2.156	4.900	3.661	2.809	
K_2	1.023	1.043	1.741	2.190	3.429	4.281	
K_3	1.623	1.487	1.890	−	−	−	T=7.090%
K_4	2.414	2.474	1.303	−	−	−	
S	2.655	3.010	0.956	4.590	0.034	1.354	

analysis of variance for the porosity ratio in the plasma-MIG welding process are listed in Table 4, which indicates that the effect of factor D is greater than those of others, the secondary is factor B, factor E, factor A and factor C in turn. S is the sum of squares of deviations; D_f is the degree of freedom; *Ms* is mean square.

Table 4 ANOVA results for porosity ratio in $L_{16}(4^4\times2^3)$ matrix

Source	*S*	D_f	*Ms* (S/D_f)	*F* [a]
A	26.55	3	8.85	3.81
B	30.10	3	10.03	4.32
C	9.56	3	3.19	1.38
D	45.90	1	45.90	19.78
F	13.54	1	13.54	5.84
e′	9.27	4	2.32	

[a] $F_{0.05}(3,4)=6.59$, $F_{0.1}(3, 4)=4.19$, $F_{0.01}(1, 4)=21.20$, $F_{0.05}(1, 4)=7.71$, $F_{0.1}(1, 4)=4.54$.

4.2 Influence of welding parameters on porosity

During the plasma-MIG welding of aluminum, stable plasma arc connected with the cathode and protecting the MIG arc, droplets and weld pool against hydrogen derived from the vapor in outer air or surface cleaning plays an important role in cleaning the plate surface so the plasma gas flow rate obviously influences the porosity ratio. When the plasma gas flow rate is below 4 L/min for 10 mm ring shaped plasma anode provided with a carbon insert, the arc column fluctuates with anode the spot moving around on the inner wall of the ring carbon, which results in poor protection. With the increase of plasma gas flow rate, arc column expands gradually and fills the constricting nozzle, a particularly rigid and stable plasma jet is obtained. ANOVA results listed in Table 4 also show that porosity ratio decreases with increasing the plasma gas flow rate. Turbulent flow often occurs and air is easily drawn into arc column with excessively high flow rate especially for high speed welding.

The influence of welding speed on porosity ratio is due to the influence of the life period of welding pool. UDA and OHNO[13] set up a model for porosity formation proceeding from the marked reduction in the solubility of hydrogen in liquid aluminum with decreasing temperature and the slow rate of ascent of gas bubbles in liquid aluminum relative to the solidification time. During solidification, the bubbles immediately trapped between the growing crystals and did not have enough time to escape from the weld pool with high welding speed, so the porosity ratio raised with the increase of welding speed, and at the same time the defects of undercut or inadequate penetration are prone to form.

ANOVA table also shows that the porosity ratio touches bottom and steps up later with the increase of MIG voltage, which may be explained that weakened surface cleaning and shortened arc length result in spatters for decrease of MIG voltage. On the other hand, swing may be caused if MIG arc is too long, which can also bring instability to destroy the effect of protection. Both of these would increase the content of hydrogen in the welding pool to form pores. The influence of wire feed rate on the porosity rate is similar with the MIG voltage, but it has little effect on the rate of plasma current which could be explained as less influences on metal transfer during plasma-MIG welding process [14−16]. Although from the ANOVA results, the effect of shielding gas flow rate on porosity rate may be negligible as compared to other factors, it does not mean that the factor has no effect at all. Turbulent flow often occurs with excessively high flow rate of shielding gas.

From the analysis of the relationship between the factors above and the porosity ratio, the optimum plasma-MIG welding process could be concluded and it is listed in Table 5.

Table 5 Optimum parameters for less porosity in plasma-MIG welding process

Wire feed rate/ ($m\cdot min^{-1}$)	MIG voltage/ V	Plasma current/ A
10.1	28.5	95−140
Plasma gas flow rate/ ($L\cdot min^{-1}$)	**Shielding gas flow rate/($L\cdot min^{-1}$)**	**Welding speed/ ($mm\cdot min^{-1}$)**
10	20−25	400

4.3 Verification tests

In order to verify the improvement of reducing porosity in the joint, confirmation experiments were conducted under the optimum conditions $A_2B_2C_2D_2E_1F_1$ and $A_2B_2C_3D_2E_1F_1$. The X-ray inspection images and macrophotographs of cross-section are shown in Fig.3 and Fig.4, respectively. The welded joins with good mechanical performance listed in Table 7 were obtained, which could reach 92.62% tensile strength and 85.12% elongation of the base metal.

5 Conclusions

1) The orthogonal test results showed that the effect of plasma gas flow rate is more dominant than other factors, the secondary factors are MIG welding voltage, welding speed, wire feed rate and plasma current in turn.

2) Confirmation experiments were conducted under optimum conditions and there was hardly any pore in the welded joint. Joints with good mechanical performance were obtained, which reached 92.62% tensile strength and 85.12% elongation of the base metal.

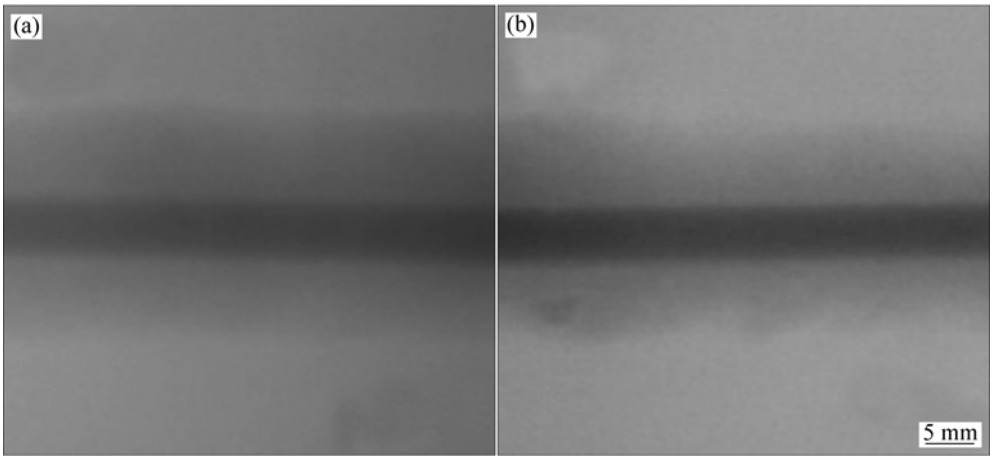

Fig.3 X-ray inspection images of samples produced under optimum conditions: (a) $A_2B_2C_2D_2E_1F_1$; (b) $A_2B_2C_3D_2E_1F_1$

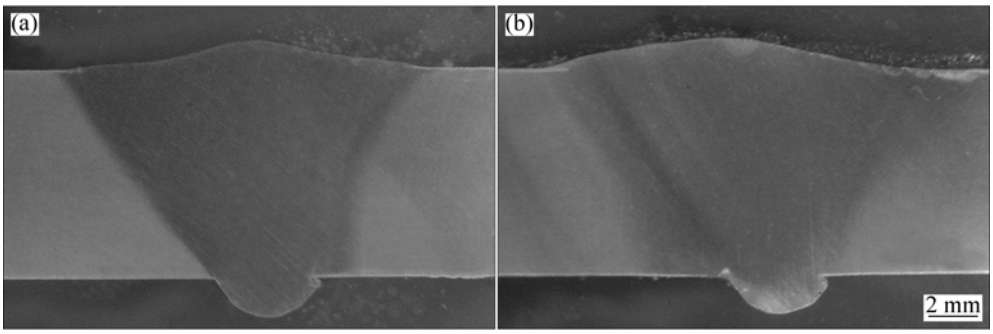

Fig.4 Macrophotographs of cross section in samples produced under optimum conditions: (a) $A_2B_2C_2D_2E_1F_1$; (b) $A_2B_2C_3D_2E_1F_1$

References

[1] ESSERS W G, JELMORINI G, TICHELAAR G W. The plasma-MIG welding process [J]. Tool and Alloy Steels, 1978, 12(8): 275−277.

[2] ESSERS W G, JELMORINI G, TICHELAAR G W. Plasma-MIG welding [J]. Philips Technical Rev, 1973, 33(1): 21−24.

[3] MAKARENKO N A, NEVIDOMSKIJ V A. Thermal cycles in plasma-MIG surfacing [J]. Automatic Welding, 2003, 1(1): 45−47.

[4] MATTHES K, KOHLER T. Electrical effects and influencing quantities in the case of the hybrid plasma-MIG welding process [J]. Welding and Cutting, 2002, 54(2): 87−90.

[5] ZHANG Yi-shun, LIU Lei; DONG Xiao-qiang, LI De-yuan. Design and development of plasma-MIG welding equipment [J]. Journal of Shenyang University of Technology, 2007, 29(2): 135−138. (in Chinese)

[6] KNOTEK O, SCHREY A. Corrosion, erosion and protection of welded structures [J]. Welding in the World, 1993, 32(1): 43−49.

[7] ESSERS W G, JELMORINI G, TICHELAAR G W. Arc characteristics and metal transfer with plasma-MIG welding [J]. Metal Construction and British Welding Journal, 1972, 4(12): 439−447.

[8] TON H. Physical properties of the plasma-MIG welding [J]. Applied Physics, 1975, 8(4): 922−933.

[9] SCHEVERS A A. Plasma-MIG welding of aluminum [J]. Welding and Metal Fabrication, 1976, 44(1): 17−20.

[10] OLIVEIRA M A, DUTRA J C. Electrical mode for the plasma-MIG hybrid welding process [J]. Welding and Cutting, 2007, 6(6): 324−328.

[11] ZHANG Yi-shun, DONG Xiao-qiang, LI De-yuan. Numerical simulation of fluid field and temperature field in plasma torch [J]. Transactions of the China Welding Institution, 2005, 26 (9): 77−80. (in Chinese)

[12] CHEN Kui. Experimental design and analysis [M]. Beijing: Tsinghua University Press, 1996: 94−102. (in Chinese)

[13] UDA M, OHNO S. Porosity formation in weld metal (Ⅰ): Effect of hydrogen on porosity formation in pure aluminum at non-arc melting [J]. Trans Nat Res Inst Met, 1974, 16(2): 433−439.

[14] BAI Yan, GAO Hong-ming, WU Lin. Plasma-gas metal arc welding procedure on low carbon steel [J]. Transactions of the China Welding Institution, 2006, 27 (9): 59−62. (in Chinese)

[15] BAI Yan. Plasma-MIG arc characteristics and welding process on aluminum alloys [D]. Harbin: School of Material Science and Engineering, Harbin Institute of Technology, 2007. (in Chinese)

[16] BAI Yan, GAO Hong-ming, WU Lin, SHI Lei. Introduction of plasma-MIG process application and welding equipment [J]. Electric Welding Machine, 2006, 36(12): 32−34. (in Chinese)

(Edited by FANG Jing-hua)